



AFRL-RX-WP-JA-2017-0194

**DESIGN AND DEMONSTRATION OF AUTOMATED
DATA ANALYSIS ALGORITHMS FOR ULTRASONIC
INSPECTION OF COMPLEX COMPOSITE PANELS
WITH BONDS (POSTPRINT)**

**John T. Welter
AFRL/RX**

**John C. Aldrin
Computational Tools**

**David S. Forsyth
TRI/Austin**

**12 July 2016
Interim Report**

**Distribution Statement A.
Approved for public release: distribution unlimited.**

© 2016 AIP PUBLISHING LLC

(STINFO COPY)

**AIR FORCE RESEARCH LABORATORY
MATERIALS AND MANUFACTURING DIRECTORATE
WRIGHT-PATTERSON AIR FORCE BASE, OH 45433-7750
AIR FORCE MATERIEL COMMAND
UNITED STATES AIR FORCE**

REPORT DOCUMENTATION PAGE				<i>Form Approved</i> OMB No. 0704-0188	
The public reporting burden for this collection of information is estimated to average 1 hour per response, including the time for reviewing instructions, searching existing data sources, gathering and maintaining the data needed, and completing and reviewing the collection of information. Send comments regarding this burden estimate or any other aspect of this collection of information, including suggestions for reducing this burden, to Department of Defense, Washington Headquarters Services, Directorate for Information Operations and Reports (0704-0188), 1215 Jefferson Davis Highway, Suite 1204, Arlington, VA 22202-4302. Respondents should be aware that notwithstanding any other provision of law, no person shall be subject to any penalty for failing to comply with a collection of information if it does not display a currently valid OMB control number. PLEASE DO NOT RETURN YOUR FORM TO THE ABOVE ADDRESS.					
1. REPORT DATE (DD-MM-YY) 12 July 2016		2. REPORT TYPE Interim		3. DATES COVERED (From - To) 3 March 2014 – 12 June 2016	
4. TITLE AND SUBTITLE DESIGN AND DEMONSTRATION OF AUTOMATED DATA ANALYSIS ALGORITHMS FOR ULTRASONIC INSPECTION OF COMPLEX COMPOSITE PANELS WITH BONDS (POSTPRINT)				5a. CONTRACT NUMBER IN-HOUSE	
				5b. GRANT NUMBER	
				5c. PROGRAM ELEMENT NUMBER	
6. AUTHOR(S) 1) John T. Welter – AFRL/RX 2) John C. Aldrin - Computational Tools <div style="text-align: right;">(continued on page 2)</div>				5d. PROJECT NUMBER	
				5e. TASK NUMBER	
				5f. WORK UNIT NUMBER X0UK	
7. PERFORMING ORGANIZATION NAME(S) AND ADDRESS(ES) 1) AFRL/RX 2) Computational Tools Wright-Patterson AFB, OH 4275 Chatham Ave 45433 Gurnee, IL 60031 <div style="text-align: right;">(continued on page 2)</div>				8. PERFORMING ORGANIZATION REPORT NUMBER	
9. SPONSORING/MONITORING AGENCY NAME(S) AND ADDRESS(ES) Air Force Research Laboratory Materials and Manufacturing Directorate Wright-Patterson Air Force Base, OH 45433-7750 Air Force Materiel Command United States Air Force				10. SPONSORING/MONITORING AGENCY ACRONYM(S) AFRL/RXCA	
				11. SPONSORING/MONITORING AGENCY REPORT NUMBER(S) AFRL-RX-WP-JA-2017-0194	
12. DISTRIBUTION/AVAILABILITY STATEMENT Distribution Statement A. Approved for public release; distribution unlimited.					
13. SUPPLEMENTARY NOTES PA Case Number: 88ABW-2016-3422; Clearance Date: 12 Jul 2016. This document contains color. Journal article published in AIP Conference Proceedings, Vol. 1706, Feb 2016. © 2016 AIP Publishing LLC. The U.S. Government is joint author of the work and has the right to use, modify, reproduce, release, perform, display, or disclose the work. The final publication is available at doi: 10.1063/1.4940591					
14. ABSTRACT (Maximum 200 words) To address the data review burden and improve the reliability of the ultrasonic inspection of large composite structures, automated data analysis (ADA) algorithms have been developed to make calls on indications that satisfy the detection criteria and minimize false calls. The original design followed standard procedures for analyzing signals for time-of-flight indications and backwall amplitude dropout. However, certain complex panels with varying shape, ply drops and the presence of bonds can complicate this interpretation process. In this paper, enhancements to the automated data analysis algorithms are introduced to address these challenges. To estimate the thickness of the part and presence of bonds without prior information, an algorithm tracks potential backwall or bond-line signals, and evaluates a combination of spatial, amplitude, and time-of-flight metrics to identify bonded sections. Once part boundaries, thickness transitions and bonded regions are identified, feature extraction algorithms are applied to multiple sets of through-thickness and backwall C-scan images.					
15. SUBJECT TERMS automated data analysis (ADA) algorithms; time-of-flight indications; backwall amplitude dropout; bond-line signal; C-scan					
16. SECURITY CLASSIFICATION OF:			17. LIMITATION OF ABSTRACT: SAR	18. NUMBER OF PAGES 14	19a. NAME OF RESPONSIBLE PERSON (Monitor) Eric Lindgren 19b. TELEPHONE NUMBER (Include Area Code) (937) 255-9806
a. REPORT Unclassified	b. ABSTRACT Unclassified	c. THIS PAGE Unclassified			

REPORT DOCUMENTATION PAGE Cont'd

6. AUTHOR(S)

3) David S. Forsyth - TRI/Austin

7. PERFORMING ORGANIZATION NAME(S) AND ADDRESS(ES)

3) TRI/Austin, Austin, 415 Crystal Creek Dr, TX 78746

Design and Demonstration of Automated Data Analysis Algorithms for Ultrasonic Inspection of Complex Composite Panels with Bonds

John C. Aldrin^{2, a)}, David S. Forsyth^{3, b)}, John T. Welter^{1, c)}

¹*Air Force Research Laboratory (AFRL/RXCA), Wright-Patterson AFB, OH 45433*

²*Computational Tools, Gurnee, IL 60031*

³*TRI/Austin, Austin, TX 78746*

^{a)} aldrin@computationaltools.com

^{b)} dforsyth@tri-austin.com

^{c)} john.welter.2@us.af.mil

Abstract. To address the data review burden and improve the reliability of the ultrasonic inspection of large composite structures, automated data analysis (ADA) algorithms have been developed to make calls on indications that satisfy the detection criteria and minimize false calls. The original design followed standard procedures for analyzing signals for time-of-flight indications and backwall amplitude dropout. However, certain complex panels with varying shape, ply drops and the presence of bonds can complicate this interpretation process. In this paper, enhancements to the automated data analysis algorithms are introduced to address these challenges. To estimate the thickness of the part and presence of bonds without prior information, an algorithm tracks potential backwall or bond-line signals, and evaluates a combination of spatial, amplitude, and time-of-flight metrics to identify bonded sections. Once part boundaries, thickness transitions and bonded regions are identified, feature extraction algorithms are applied to multiple sets of through-thickness and backwall C-scan images, for evaluation of both first layer through thickness and layers under bonds. ADA processing results are presented for a variety of complex test specimens with inserted materials and other test discontinuities. Lastly, enhancements to the ADA software interface are presented, which improve the software usability for final data review by the inspectors and support the certification process.

INTRODUCTION

The ultrasonic inspection of aerospace composites has been demonstrated to be one of the most effective methods to detect critical defect types and ensure the reliability of composite structures [1-3]. Most inspection applications of composites and bonded joints are based on pulse-echo ultrasonic testing (UT) and manual C-scan data interpretation. Using amplitude and time-of-flight C-scan data, delaminations, disbonds, porosity, and foreign materials can be detected and located in depth. However, the ultrasonic inspection of large composite structures requires significant manpower and production time. To address this inspection burden and ideally increase inspection reliability, software tools and automated data analysis (ADA) algorithms [4-9] have been developed to support the assessment of ultrasonic data from composite components. Recent work on the design of ADA algorithms [7-9] follows standard procedures for analyzing signals for time-of-flight indications and backwall amplitude dropout. However, certain complex composite structures with varying shape, thickness transitions and the presence of bonds can greatly complicate this interpretation process.

Most prior work concerning the inspection of bonded regions in composites has focused on bond integrity [10]. The topic of detecting discontinuities and characterizing complex composites parts with bonded components and ply drops has received some recent attention on enhanced ultrasonic NDE techniques [11-13]. An example test panel with a bonded pad-up region is shown in Fig. 1. Frequently, the edges of adhesive layers are found at thickness transitions,

producing multiple shifting signals and coherent noise in the pulse-echo UT data, resulting in a challenging signal interpretation task. In this paper, enhancements to the automated data analysis algorithms are introduced to address these challenges. One requirement is to estimate the thickness of the part and presence of bonds without prior information. This task is accomplished by tracking potential backwall signals, detecting the presence of multiple signals and step changes which indicate bonded sections, and through the application of smart spatial filters for estimating the panel thickness and additional bonded sections with varying signal levels. Once part boundaries, thickness transitions and bonded regions are identified, feature extraction algorithms are applied to multiple sets of through-thickness and backwall C-scan images, for evaluation of both first layer through thickness and layers under bonds. In this study, a challenge set of test data was selected to verify the ADA algorithms over a wide range of complex parts and artificial defects located both above and below the bond-line, as shown in Fig 1.

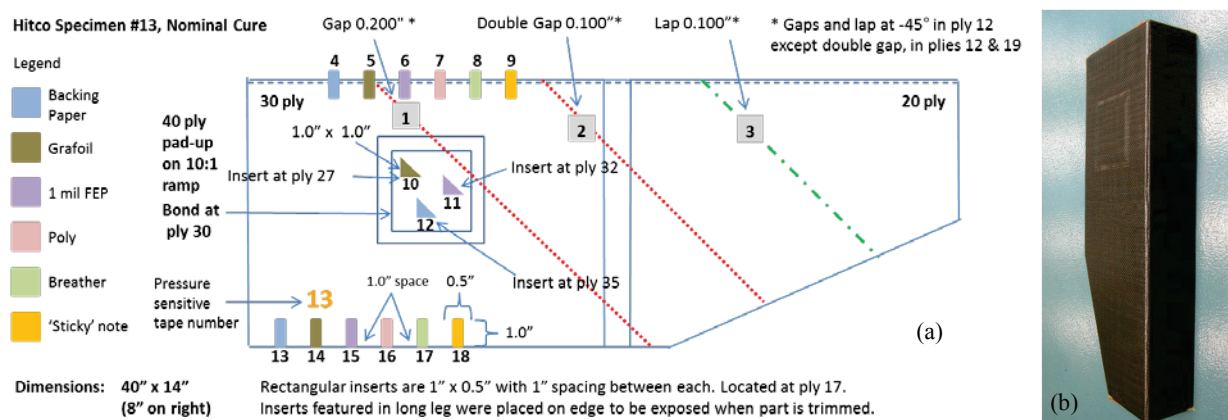


FIGURE 1. (a) Diagram and (b) photo of Hitco test panel #13 with a bonded pad-up region and inserted materials.

AUTOMATED DATA ANALYSIS ALGORITHM DESIGN FOR BONDED REGIONS

The design objective for the software is to make calls on all anomalous indications that satisfy the inspection criteria while minimizing false calls associated with normal part conditions. Anomalous indications studied in this program include inserted materials, porosity, ply ‘laps and gaps’, and wrinkles. Inserted materials may occur during manufacturing, possibly originating from such items as backing paper, glove (poly), breather or miscellaneous factory materials. Other artificial materials like Grafoil, FEP and ‘sticky’ notes have been used for testing purposes and can produce challenging ultrasonic inspection conditions for demonstration tests. Shapes of inserted materials may be triangular (e.g. corners of backing paper), rectangular or more irregular shapes. A minimum dimension criterion for an indication is typically defined with the test specification. Often, 0.25" x 0.25" (0.63 cm x 0.63 cm) squares are prescribed as minimum dimensions for inserted materials. There are a number of potential false call features that should ideally be vetted by any automated data analysis algorithm as an operator would. Such part features include edges, ply drops, panel radii, stringers / beam-type structures, and noodles at radii. Operators typically use knowledge of the part and a view of the TOF C-scan image to distinguish part features from an amplitude drop-out due to anomalous conditions. Lastly, scanning artifacts such as streaking, water on the part, or scanner backlash may also be present in ultrasonic data and can be easily rejected by a trained operator.

The base ADA algorithm process steps were first described in prior work [7-9]. The proposed automated data analysis approach strives to automate the entire ultrasonic data analysis process including the creation of the C-scan amplitude and TOF images to make indication calls. The current design of the ADA algorithm does require access to the full A-scan data acquired for the part, which might be a limitation for some older UT systems. Building on the prior designs, the following steps will emphasize algorithm updates to enhance detection capability of regions with bonds and adjacent thickness transitions, and minimize the false call rate.

(a) Evaluate calibration data. The first step is to evaluate the inspection system using calibration data acquired from a known reference standard. A signal-to-noise acceptance criterion is evaluated for the back wall signal with respect to the internal noise echoes (e.g. 20 dB SNR) to ensure the transducers are operating properly. Call performance on known defects in the reference standard must also be verified. One change from prior work is calling

‘sub-rejectable’ indications, under the dimension and area criteria. Some of the inserted material indications in standards do not always meet the strict dimension criteria; however, verification of these indications is important.

(b) Process front-wall signals and identify part edges. The front-wall (FW) C-scan is used to locate the part domain and edges. By evaluating the edge locations and applying the inspection zone criterion for distance from edges (for example, 1.0 in), a map identifying the different inspection zones can be created. The algorithm calls three zones: an *acreage region* away from the edges in the part, and *edge region* based on the edge criterion, and a thin *buffer region* that is within roughly 0.24" (typically 3 pixels) of where the FW signal drops off. A buffer region is applied in order to avoid false calls in the edge region due to a lack of consistent backwall signals at the part edge. The FW signals also provide a means to check that signal levels are adequate, which was found to reduce false calls.

(c) Evaluate signal width for setting the start and end of gates. The front-wall signals are used to evaluate the pulse width during inspection. Since gates must be automatically set by the ADA algorithm to produce internal and backwall C-scan images, it is important to have a precise measure of how the signals rise and ring down in time in order to avoid false calls. More details on this process can be found in prior work [9].

(d) Identifying bonds in test parts. Improving calls in bonded sections of production parts requires detecting their location and extent. From the perspective of pulse-echo ultrasound, both the bond-line and the backwall signal produce reflections, somewhat smaller in magnitude than regular backwall signals without an adhesive layer present. The first challenge here is distinguishing regions with bonds from specimens with strong multiple reflections often from thin panel regions. As well, signal from bond-line does not always meet criteria for a backwall signal, as shown in the TOF C-scan image in Fig. 2(a). To evaluate the regions, signals are tracked before and after the 1st backwall / bond-line signals as shown in Fig. 2(b) and Fig. 2(c) respectively. This provides a rough map of the missing TOF signals in Fig. 2(a). Then, clustering routines with a minimum area criteria is applied to group regions of multiple potential ‘backwall’ signals. Next, two signal metrics are evaluated for each multi-signal region, shown in Fig. 3, to distinguish regions with bonds and thin multi-layer structures. The first metric (x-axis) compares the ‘time-of-flights’ of multiple signals and normalizes the time difference with respect to 1/2 of the second signal. Signals due to multiple reflections in a single layer will have a value near 0. The second metric (y-axis) quantifies the change in amplitude of signals. It has been observed that bond signals and backwall signals under bonds are close in amplitude, versus multiple reflections in a layer which exhibit significant decay. Figure 3 presents results for these two metrics for a number of examples of bond data and thin layer composite data. A simple linear classifier can be used to call *regions with bonds* with good reliability.

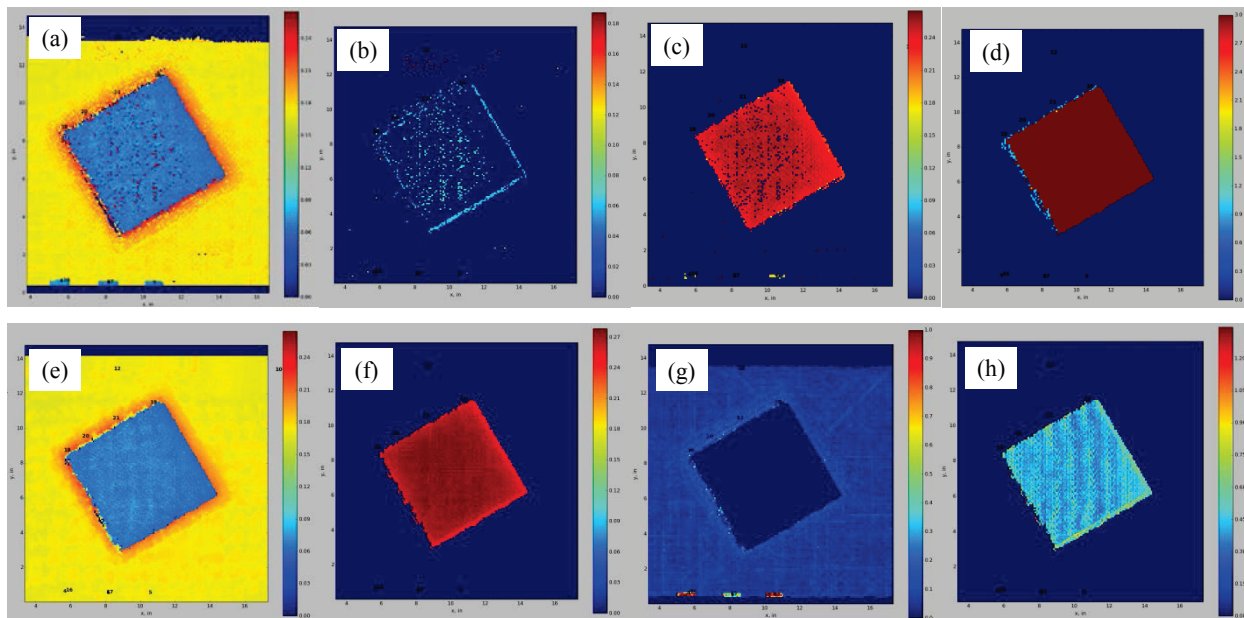


FIGURE 2. C-scan images showing bond detection and interpretation process: (a) initial backwall TOF C-scan estimate, (b) TOF maps (b) before and (c) after estimated ‘backwall’ signal, (d) called bond region (red) with include edge pixels (light blue), (e) revised backwall TOF C-scan map with complete bond, (f) backwall TOF C-scan under bond, (g) C-scan amplitude plot for internal gate (for TOF+ calls), and (h) C-scan amplitude plot of backwall signal under bond (for BW2 calls).

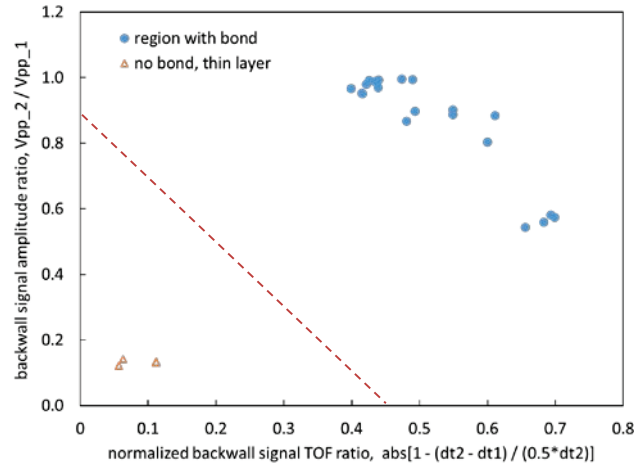


FIGURE 3. Comparison of time-of-flight and amplitude ratio metrics for a sample of ‘no bond’ and ‘with bond’ regions.

(e) Estimate backwall and bond-line depth using enhanced backwall search process. To identify the features in the C-scan amplitude map, simultaneous interpretation of the C-scan TOF map is needed to distinguish internal and backwall signals. Thus, an accurate assessment of the true backwall depth and depth of multiple layers due to bonds over the entire part is needed. In prior work, a smart ‘backwall’ search process for the TOF C-scan map was introduced [9]. Recent improvements to this process have been made by using current state-of-the-art in-painting algorithms [14] providing greater accuracy in estimating the backwall level under regions with defects, complex ply drops, surface curvature and general poor data quality (e.g. data dropout). However, this backwall estimation process is complicated by the presence of bond regions with a second ‘true’ backwall signal. Ultrasonic scans are presented in Fig. 4 contrasting the response for inspections from the tool side and bag side of the panel #13 pad-up region including the bond. Often, there is an abrupt transition from the backwall (shifting deeper) to where an adhesive layer is being detected earlier in time, as shown in Fig 4(c) and Fig 4(d). When *regions with bonds* are present, the backwall estimation process is broken into separate steps with masks, first outside, then inside for each identified bonded region. An iterative process was then implemented for tracking disconnected signals at the edge of the adhesive layers, improving backwall tracking. This process was able to reduce false calls in thickness transitions neighboring bonded

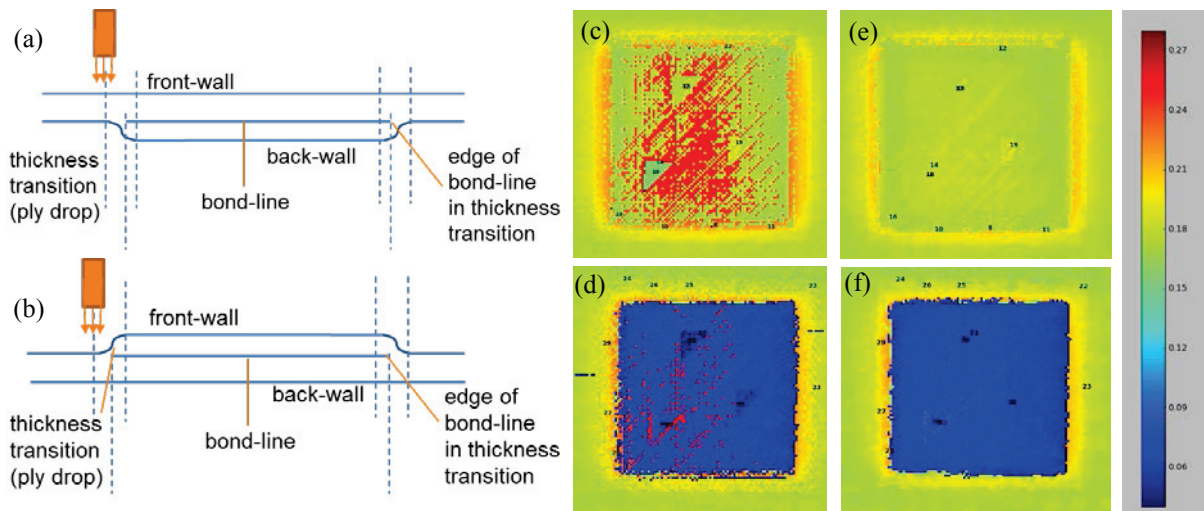


FIGURE 4. Ultrasonic scan from (a) tool side and (b) bag side of pad-up region with an adhesive bond. Signals from the edge of the bond-line signal in (c) and (d) can produce early ‘through thickness’ indications in time in the composite thickness transition zone. Results for the refined backwall and bond-line estimates are presented for the (e) tool side and (f) bag side.

regions. However, some further refinements may still be needed. For example, the edges of bonded regions are still the biggest area of false calls. One can easily set up a criteria to remove most of these based on their proximity to the edge of an adhesive layer plus a thickness transition. Much more ‘noise’ also appears to be present between the front-wall and adhesive layer. However, at this time, it was chosen to be more sensitive to ensure no significant defects are missed. TOF map results for the pad-up region in Hitco panel #13 using the ‘enhanced’ backwall search for the 1st level and 2nd level (backwall signal under bonds) are shown in Fig. 2(e) and Fig. 2(f) respectively.

(f) Identify part zones and transitions. Due to the presence of ramps, stringers and radii changes in composite parts, this interpretation task can become complicated. By using the front wall amplitude C-scan image and the estimated backwall TOF map, the different region types can be classified. The following inspection zone categories are identified using the front-wall / edge metric map: (0) off-part, (1) acreage zone (away from edge or radii), (2) edge zone, (3) backwall thickness transition zone, and (4) region with a bond. In the ADA software interface, metrics are now being presented to the user for each called indication whether that location meets the criteria for an edge (*Cedge*), a thickness transition (*Ctrans*) and a region with a bond (*Cbond*). Values that exceed the criterion for each category are highlighted in ‘yellow’. Examples are shown in Fig. 5 and 6 with indications for the three part zone metrics.

(g) Create internal signal C-scans and evaluate noise level for part. A through thickness internal ‘only’ signal C-scan can be generated following the front-wall signal and using a backwall follower with the estimated backwall signal TOF map. Internal signals above a threshold level are then called to produce an internal indication C-scan map (TOF+) with binary values. An example around a bonded region is shown in Fig. 4(g). Improved detection reliability and reduced false call rate were achieved through adapting the base threshold level with respect to the measured internal noise level within the gate [9].

(h) Create backwall signal ‘only’ C-scans. Using the TOF map for the backwall signal with a tight gate, a backwall signal ‘only’ amplitude C-scan can be generated. Loss of backwall signals below a prescribed threshold level is then called to produce a backwall loss C-scan map (BW-) with binary values. Adaptive call criteria have also been applied to address sensitivity to variation in backwall signal level observed in the wide range of test data studied to date [9].

(i) Perform feature extraction and classification of internal (TOF+) signals. Feature extraction algorithms can now be applied to the internal indication C-scan map (TOF+). Contour finding algorithms are then applied and clustering is used to combine closely spaced indications, and area and dimension metrics are evaluated for all significant clusters. The location of each cluster is assessed with respect to the inspection zone maps in order to ensure it is evaluated using the correct inspection zone criteria. All indications that satisfy the amplitude, dimension and area criteria are recorded along with the call metrics and identified inspection zone.

(j) Perform initial feature extraction and classification of backwall signal loss (BW-) and signal loss under bonds (BW2): The C-scan amplitude plot for the backwall signals can be gated to create a binary map of backwall signals below a threshold (BW-) and backwall signals under bonds (BW2). Again, contour finding algorithms are then applied and clustering is used to combine closely spaced indications that satisfy the minimum area metric requirements. The location of each cluster is assessed with respect to the inspection zone maps in order to ensure it is evaluated using the correct criteria. All indications that satisfy the amplitude and area criteria are recorded along with the call metrics and identified inspection zone.

(k) Generate porosity criteria map and perform evaluation (BWp). To perform the porosity evaluation, the backwall C-scan TOF map can be transformed into an attenuation map for setting the acceptance criteria as a function of depth. The C-scan amplitude plot for the backwall signals can then be gated using the corresponding porosity criteria map threshold to create a binary map with porosity indications (BWp). A sweep algorithm is used to identify regions of the part that exceed the porosity area criteria and within the region size requirement (for example, 25% pixels meeting the acceptance criteria over a 1.0 in. square region.) At this stage, a cluster search algorithm (as applied to the TOF+ and BW- indication map) groups neighboring regions from the porosity (BWp) indication map.

(l) Evaluate TOF thickness indications (TOF2). Often, delaminations or foreign material located in the first few plies can be difficult to detect using either internal defect gating or backwall dropout metrics. However, internal time-of-flight plots can often provide clear indications of such features. The current algorithm applies a change in time threshold from the backwall to form the indication map (TOF2). The cluster search and size evaluation process is applied here to verify such indications satisfy the acceptance criteria. Enhancements to the algorithm have been implemented to address panel-to-panel thickness variation and thickness ‘noise’ at transitions. For more info, see [9].

(m) Compile calls with metrics. Indications with call metrics are presented to the operator. These include called indication type (TOF+, BW-, BWp, TOF2, BW2), indication size (length, width, and area), median signal level (in dB) with respect to the call criteria, and zone metrics (*Cedge*, *Ctrans* and *Cbond*). Progress has been made to sort calls based on likelihood of the indication being a significant defect, based on these metrics and grouped by call type.

RESULTS FOR TEST PANELS WITH BONDED REGIONS

An example of ADA processing results is presented for the test specimen #13 as shown in Fig. 1. This specimen contains artificial defects that have been added at varying locations and ply depth, including above and below the adhesive layer. Diagrams are shown in Fig. 4 of the ultrasonic scan of the (a) tool side and (b) bag side of pad-up region with the bond. Example ADA toolkit interface results are presented in Fig. 5 and Fig. 6 scanned from tool side and bag side respectively. In the first column of the results windows, a code is used to describe what criterion was met to make the call: (TOF+) amplitude C-scan of internal signals, (BW-) C-scan of backwall dropout, (TOF2) TOF C-scan internal signals, and (BW2) C-scan of backwall dropout under a bond. Indications are listed in the spreadsheet display in the upper left and corresponding numbers are presented identifying the indications in the C-scan image display on the right. For these ADA evaluations for the two different scan orientations, the three triangular inserts in the bond region were all correctly called. For the tool side scan (Fig. 5), the left most triangle is in front of the bond, while the right two triangle are behind the bond. The left triangles were called by TOF2 and BW2 algorithms, while the right triangle was only called by BW2. For the bag side scan (Fig. 6), the left most triangle is behind the bond, while the right two triangle are in front of the bond. This left most triangle was called using both the BW2 and TOF2 criteria. Examples of the backwall signal loss maps under the bonds are shown in Fig 7. While the signal loss is clearly observed with the presence of the triangular inserts, in a few cases, the drop for the right triangle in Fig. 7(b) may not quite meet a fixed call criteria. Note, this indication was called by the TOF2 algorithm. Thus, there are benefits of using multiple call criteria in these bonded regions. As well, adapting the call criteria for BW2 indications as a function of the bond and backwall signal quality would ensure more reliable calls for varying part conditions.

Note, in both Figures 5 and 6, some false indications are displayed, nearly all due to backwall loss indications at edges and transition regions with bonds present that satisfy the call criteria. While operator review can quickly reject these indications, a key objective is to improve the performance of the ADA software for rejecting such indications. Refinements have been made to minimize these calls over a wide test set including a number of panels with bonds scanned from different sides and varying gain levels.

Lastly, indications for the six inserted materials at the radii are also observed in the TOF map in Fig. 5 and 6. However, the inserted 'sticky' note material was found to have the weakest response by far. Unfortunately, the signal dimensions and area do not meet the call criteria in these two cases. It appears that the paper material of the 'sticky' note is prone to being saturated with resin during cure, and produces much weaker responses than the other five inserted test materials. Careful finger-printing of 'sticky' note defects is needed to properly test the ADA algorithms.

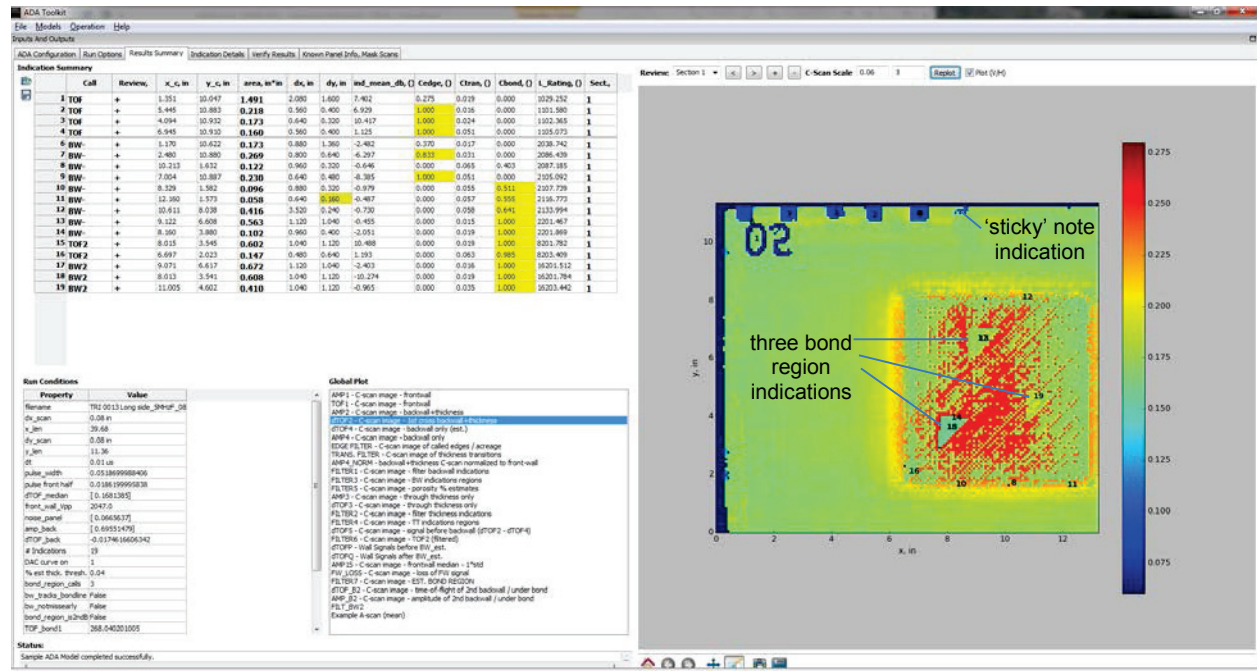


FIGURE 5. Example ADA toolkit interface results for Hitco test panel #13, scanned from tool side, with TOF C-scan view.

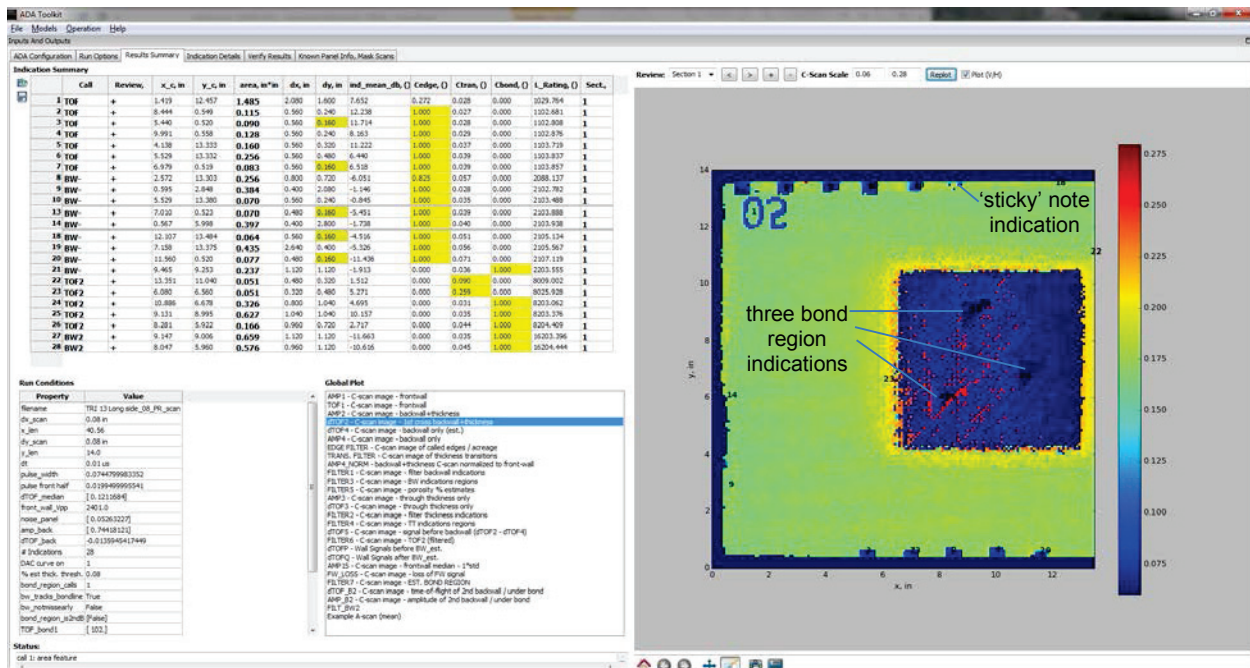


FIGURE 6. Example ADA toolkit interface results for Hitco test panel #13, scanned from bag side, with TOF C-scan view.

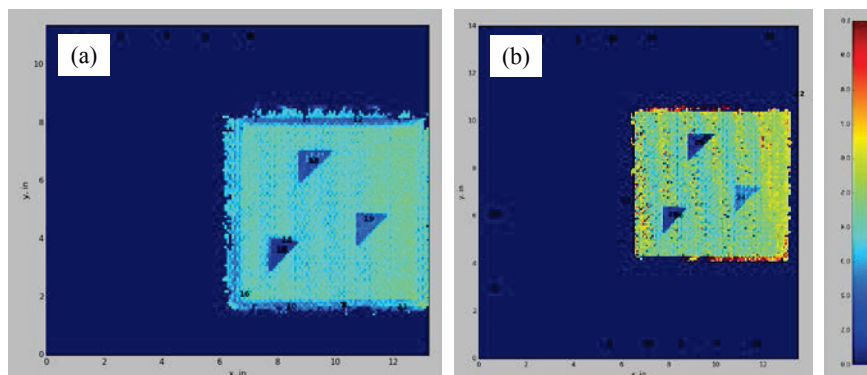


FIGURE 7. C-scan of backwall loss under the bond-line with three triangular inserts for (a) tools side and (b) bag side scans.

SOFTWARE TOOLS FOR DATA REVIEW AND TO SUPPORT CERTIFICATION

A software interface for the automated data analysis (ADA) toolkit has been presented in Fig. 5 and 6. The *ADA Toolkit* is a component of the open-source *NDI Toolbox™* led by TRI/Austin. The main view provides a summary of the found indications in the analyzed data, a visual presentation of an indication map and quantitative metrics assisting the operator in understanding why each call was made. The software uses a modular approach to designing and transitioning ADA algorithms. The *ADA Toolkit* ‘plug-ins’ consist of a configuration file and the analysis code that can be imported within the interface. Python is the base programming language for the ADA algorithm code. The ADA algorithms have also been parameterized with values stored in the configuration file such that the acceptance specifications can be modified within the software for a new part or inspection procedure. A configuration viewer is provided within the user interface for modifying all of the parameter settings for the ADA algorithm. A design goal is to create a tool that can be easily adapted by expert operators following test specimen acceptance criteria for different composite material types, thicknesses and ideally part complexity. To support the operator review of indications, the

ADA Toolkit provides an indication viewer, to review quantitative metrics, image and signal data, and qualitative call descriptions for each indication. For more information on the software interface design, see reference [7-9].

Software features have also been integrated into the ADA Toolkit to facilitate algorithm design and parameter optimization studies, and support certification. The software can run a set of UT files in batch mode, process the results, compare them to truth tables for each file, and compile the total correct call, missed call, and false call rates for the set. Features have been transitioned to import 'truth' tables and match known flaws with the ADA generated indication table results (.ind file). An indication comparison file can be generated which organizes all of the ADA called indications into three groups: true positives (TP), missed calls (MC) and false calls (FC). Note, an indication position error factor is currently set to 0.63 cm (0.25"), providing some practical flexibility in matching ADA indications with the truth table. The output report from this process is expected to be quite useful for both parametric studies for code optimization, verifying performance with calibration panels, and quantitatively demonstrating validation for certification.

VERIFICATION TEST RESULTS

The test panel demonstrations presented in prior work [8-9] and in previous sections for panels with bonds do provide a good first step to support the use of ADA algorithms for NDE data review. However, in order to certify the use of ADA algorithms for the review of production ultrasonic NDE data from composite inspections, (1) the detection capability for the desired target size(s), (2) the rate of false calls, and (3) ideally the time difference for NDE inspector secondary review of ADA reported results (with respect to making the same calls through a manual data review) must be evaluated quantitatively. In order to evaluate the true positive (TP), missed call (MC) and false call (FC) rate of the ADA algorithms with statistical rigor, software tools were developed to automatically perform the study.

A tedious but critical step is the creation of 'truth' tables with very accurate information for all the flaws in each scan, including dimensions and locations. For an initial test study, 'truth' tables (as .csv files) were created for 40 selected Mistras and TRI/Austin UT data files from project test panels and select Hitco calibration panels. These data sets and truth tables contain over 400 insert materials indications and natural indications associated with porosity. They also include all of the toughest test panel cases such as saturated 'sticky' note inserts and partially scanned inserts at the radii. Wrinkles, laps and gaps have also been included in the truth table, but detection rates for these flaws are calculated separate from inserts and natural indications associated with porosity. In addition to the 40 panel set presented in prior work [9], a separate intermediate set of test data was selected to challenge the ADA algorithms that includes a wide range of complex parts with bonds and artificial defects located both above and below bond lines. It is critical to design a test set that provides the widest array of part and flaw characteristics that represent the expected range of data NDE inspectors review daily while also including a statistically significant number of flaw indications. For comprehensive certification, a significant number of production panels should be tested as well, ideally with some actual verified indications.

Statistical results are presented in Table 1 for the 40 challenge test files. For this study, the accuracy target was to detect 0.25"x0.25" (0.63 cm x 0.63 cm) inserts. In a POD evaluation, the goal is to assess the detection capability for the accuracy target. With a scan resolution of 0.080"x0.080" (2 mm x 2 mm), such inserts are expected produce 3 pixels in the x- and y-scan directions. Because of this criteria, the correct 'insert' calls (TP = true position) were grouped by flaw size into the three categories: (1) $TP > 0.25''sq$ (square) inserts, (2) $\%TP = 0.25''sq$ inserts and (3) $\%TP < 0.25''sq$ inserts. Past results from ref. [9] are included in the first column and new results from recent revisions of the ADA algorithm are presented in the next four columns. For the baseline Case 1, most of the 17.6% misses for 0.25''sq inserts were associated with the Nacelle test panels, where the pixel area criteria was not always met. Through a series of algorithm improvements discussed in this paper, significant improvements were made in terms of the missed call rate (Case 5): (1) $TP > 0.25''sq = 98.1\%$, (2) $\%TP = 0.25''sq$ inserts = 90.2% and (3) $\%TP < 0.25'' = 44.4\%$. One topic that was explored was the effect of calling 'sub-rejectable' indication. For Case 4, indications were called having only two pixels in width in either the dx or dy dimensions (while meeting the same area criteria of 8 pixels at 0.080" scan resolution). Some improvements were achieved in detecting previously missed calls including a wrinkle. However, the false call rate did increase by 26%. When such indications are presented to the operator in the user interface, a yellow highlight is applied to the length or depth to indicate dimensions under the criteria (see Fig. 5 and 6.) Note, four large misses still remain in the test set. These are solely dependent upon the shape and area call criteria not being met. Two of the four misses are due to saturated 'sticky' note triangles, one is due to a weak poly triangle (that can be called by modifying the *BW*- call criteria parameter) and one is due to an insert only partially scanned at the radii edge. Calling sub-rejectable *BW*- and *TOF*+ indications in signal level is being considered to help.

Because of the complexity of some of the composite test specimens, there have been challenges to reducing the number of false calls in prior work [9] as shown in Case 1. Significant progress has been made to eliminate these false calls through properly addressing the review of ultrasonic signals from bonds, an enhanced backwall tracking algorithm, taking care in making calls when the front-wall signal is weak in magnitude, and through the use of adaptive thresholding based on panel noise levels. As well, careful expert review of all of the indications was performed for the 40 panel set. Through this review process, a number of natural indications were discovered associated with porosity and wrinkles. The updated results presented in Case 3 (wrt Case 1) show a nearly 62% reduction in the false call rate for the 40 panel set, while new indication calls (TP) are also being made. By breaking out the calls as shown in Table 1, the algorithm source of the many of the true positive and false calls can be identified. Interestingly, the backwall loss criteria only contributes to call roughly 8.4% of the inserts but generates in over 60% of the false calls at thickness transitions. One observation (separate from this 40 panel study) from production part data is that BW-false calls are extremely rare compared to this 40 panel test set. Much of these backwall loss indications exist because of tape on the part edges, water on the back side of the part, or the orientation of the probe relative to the curved part surface. False calls of greater interest and challenge are associated with the TOF2 calls at the edge of bonds at thickness transitions. Some examples are found in Fig. 5 and 6 and these indications are also observed in production data. Adapting the TOF2 call criteria as a function of location should reduce these remaining false calls in Case 5.

TABLE 1. Results for 40 panel test set. Metrics include true positive (TP) detections, false calls (FC) and missed calls (MC).

	Case 1	Case 2	Case 3	Case 4	Case 5
	Ref. [9]	Rev. 7/2015a	Rev. 7/2015a	Rev. 7/2015a	Rev. 7/2015b
area threshold (# pixels, 0.08" scan res.)	8	8	8	8	8
dimension threshold (# pixels, 0.08" s.r.)	3	3	3	2	2
thrsh2, for BW- calls (dB drop)	-13.0	-13.0	-13.0	-13.0	-13.0
TP	337	344	365	368	370
MC	49	42	37	34	32
FC	263	191	100	126	119
Area (sq in.) per false call	46.7	64.2	122.7	97.4	103.1
%FC_TOF+	14.5%	20.9%	4.0%	6.4%	8.4%
%FC_BW-	59.7%	41.4%	62.0%	57.1%	60.5%
%FC_BWp	0.0%	0.0%	0.0%	0.0%	0.0%
%FC_TOF2	25.9%	30.9%	34.0%	36.5%	31.1%
%FC_BW2	NA	6.8%	0.0%	0.0%	0.0%
MC>0.25"sq inserts / porosity	4	5	6	4	4
MC=0.25"sq inserts / porosity	25	20	14	14	13
MC<0.25"sq inserts / porosity	13	13	10	10	10
%TP>0.25"sq inserts / porosity	98.1%	97.6%	97.1%	98.1%	98.1%
%TP=0.25"sq inserts / porosity	82.4%	85.9%	90.2%	90.2%	90.9%
%TP<0.25"sq inserts / porosity	27.8%	27.8%	44.4%	44.4%	44.4%
%TP_TOF+ only	25.5%	26.2%	24.1%	23.4%	23.5%
%TP_BW- only	13.7%	9.3%	8.2%	8.4%	8.4%
%TP_TOF2 only	25.2%	25.9%	29.6%	28.5%	28.4%
%TP_multiple calls	35.6%	38.7%	38.1%	39.7%	39.7%
MC, wrinkles, laps and gaps	4	4	7	6	5
TOTAL, wrinkles, laps and gaps	17	17	32	32	32
%TP, wrinkles, laps and gaps	76.5%	76.5%	76.5%	81.3%	84.4%
Expert Review of False Call Indications			✓	✓	✓

CONCLUSIONS AND FUTURE WORK

In this paper, enhancements to the automated data analysis algorithms are introduced to address the challenges of inspecting complex panels with varying shape, ply drops and the presence of bonds. One requirement was to estimate the thickness of the part and presence of bonds without prior information. This task was accomplished through tracking potential backwall signals, detecting the presence of multiple signals and step changes which are indicators of bonded sections, and through the application of smart spatial filters for estimating the panel thickness and additional bonded sections with varying signal levels. Once part boundaries, thickness transitions and bonded regions are identified, feature extraction algorithms are applied to multiple sets of through-thickness and backwall C-scan images, for evaluation of both first layer through thickness and layers under bonds. A challenge set of test data was selected to verify the ADA algorithm performance over wide range of complex parts and artificial defects located both above

and below bond lines. Today, the detection performance appears to satisfy the current target requirements for 0.25" sq. inserted materials while the false call rate is now considered reasonable. Lastly, improvements to the ADA software interface were presented, which improve the software usability with the NDI operator in data review.

At this stage, the certification process has been defined [15] and is being followed to ensure the performance of the ADA software with operator data review meets the acceptance criteria. The integrated software tools will be quite valuable to certify the use of ADA algorithms for (1) the detection capability for the desired target size, (2) the rate of false calls, and (3) the time for NDE inspector secondary review of ADA reported results. Future work is expected to further refine the evaluation as additional test data are introduced to the software. Ideally, the ADA algorithm should be optimized with all three metrics in mind. The use of prior part information on panel thickness and bond location is also being considered which could simplify this evaluation process. Software tools have been implemented to identify part information from the filename and directory encoding. Initial demonstrations have been made where part type is identified and key meta-data like part thickness and defect maps are stored and tracked over time.

ACKNOWLEDGMENTS

Support for this program was provided through the Defense-Wide Manufacturing Science and Technology Program. NDT support and test specimens for the program were provided by Jeff Kearns, Lori Witt, Gerry Taccini, Jake Stavana, Dominic Calamito and Leslie Cohen of Hitco Carbon Composites Inc. Experimental data presented here from the test specimens was provided by Mark Keiser, Jennifer Flores-Lamb and Mark Warchol of TRI/Austin Inc. and Valery Godinez-Azcuaga, Manny Butera, Alireza Farhidzadeh, Obdulia Ley, Thomas Valaka of Mistras Group Inc. Feedback on a generic test sample acceptance criteria for composite inspections and porosity evaluation was provided by Richard Bossi, Gary Georgeson, Doug Frisch, and Hong Tat of the Boeing Company. Recent support on UT data review and algorithm certification requirements has been provided by Mark Osterkamp of PAR Systems, Paul Acres and Willie Chu of Lockheed Martin, and Matt Grant and Greg Wetsig of Northrup-Grumman Technical Service. More info on the *NDI ToolboxTM* can be found at <http://ndetoolbox.com/>.

REFERENCES

1. Bar-Cohen, Y., "NDE of fiber-reinforced composite materials--A review," *Materials Evaluation*, **44**, 446-454 (1986).
2. Bossi, R. H., "NDE developments for composite structures," in *Review of Progress in Quantitative Nondestructive Evaluation*, eds. D. O. Thompson and D. E. Chimenti, (American Institute of Physics 820, Melville, NY) **25**, 965-971 (2006).
3. Smith, J.P., and Shark, L.K., "Nondestructive testing and evaluation of composite aerospace structures," *Wiley Encyclopedia of Composites*, (2012).
4. Perez, C., Fernandez, F., Borrás, M., de los Reyes, S. S., "Automatic analysis of UT inspections in aircraft structures (MIDAS-AUTODET software)," ECNDT 2006, <http://www.ndt.net/article/ecndt2006/doc/P13.pdf>.
5. Smith, R. A., and Nelson, L. J., "Automated analysis and advanced defect characterisation from ultrasonic scans of composites," *Insight – Journal of the British Institute of NDT*, **51**(2), 82-87 (2009).
6. Barut, S., Bissauge, V., Ithurralde, G., Claassens, W., "Computer-aided analysis of ultrasound data to speed-up the release of aerospace CFRP components," 18th World Conference on Nondestructive Testing, (Durban, South Africa, 16-20 April 2012), http://www.ndt.net/article/wcndt2012/papers/667_wcndtfinal00669.pdf.
7. Aldrin, J. C, Coughlin, C. R., Forsyth, D. S., Welter, J. T., "Automated data analysis algorithms and software for ultrasonic inspection of composites," SAMPE 2013 Proceedings, (Long Beach, California May 6-9, 2013).
8. Aldrin, J. C, Coughlin, C. R., Forsyth, D. S., Welter, J. T., "Progress on the development of automated data analysis algorithms and software for ultrasonic inspection of composites," in *Review of Progress in Quantitative Nondestructive Evaluation*, eds. D. E. Chimenti, L. J. Bond, and D. O. Thompson, (American Institute of Physics 1581, Melville, NY) **33**, 1920-1927 (2014).
9. Aldrin, J. C, Forsyth, D. S., Welter, J. T., "Progress on automated data analysis algorithms for ultrasonic inspection of composites," in *Review of Progress in Quantitative Nondestructive Evaluation*, eds. D. E. Chimenti and L. J. Bond, (American Institute of Physics 1650, Melville, NY) **34**, 1091-1101 (2015).
10. Adams, R. D., and Cawley, P. "A review of defect types and nondestructive testing techniques for composites and bonded joints," *NDT International*, **21**(4), 208-222 (1988).

11. Sugimoto, S., Aoki, Y., Hirano, Y., and Nagao, Y. "A study on nondestructive inspection for VaRTM composite wing structure," 16th International Conference on Composite Materials, (2007).
12. Smith, R. A. "Composite defects and their detection," *Materials Science and Engineering*, **3**, 103-143 (2009).
13. Smith, R. A., and Nelson, L. J., "Ultrasonic tracking of ply drops in composite laminates," in *Review of Progress in Quantitative Nondestructive Evaluation*, Vol. 35, AIP, (to be published 2016).
14. Telea, A. "An image inpainting technique based on the fast marching method." *Journal of Graphics Tools*, **9**(1), 23-34 (2004).
15. Welter, J. T., Aldrin, J. C, Forsyth, D. S., "Certification and implementation of an automated data analysis algorithm," in *Review of Progress in Quantitative Nondestructive Evaluation*, Vol. 35, AIP, (to be published 2016).